



## A Mechanical Model to Predict the Initial Stiffness of The Beam-to-Upright Connection in A Steel Pallet Racking System

Mohamed Yehia<sup>1,\*</sup>, Sameh M. Gawwan<sup>1</sup> and Mohamed M. Yehia<sup>1</sup>

<sup>1</sup> Civil Engineering Department, Faculty of Engineering–Mataria, Helwan University, Egypt

\*Corresponding Author E-mail: [Mohamedyehia96@m-eng.helwan.edu.eg](mailto:Mohamedyehia96@m-eng.helwan.edu.eg)

### Abstract

Pallet racking systems are a mainstay of contemporary logistics and warehousing operations, offering effective storage solutions to a variety of global sectors. The rotational stiffness of the beam-to-upright connection of the pallet racking system is very important for the design of any finite element program. This paper introduces a mechanical model, employing the component method, aimed at predicting the initial rotational stiffness of beam-to-upright connections within cold-formed steel storage racks. An experimental investigation of the behavior of beam-to-column connections in a steel pallet racking system is conducted, and the results are used to verify the mechanical model. The findings indicate that there is a satisfactory agreement between the experimental results and the initial rotational stiffness values derived from the mechanical model.

**Keywords:** Rotational stiffness; Steel pallet racking system; Cold-formed steel; Semi rigid connection; Beam to column connection; Single cantilever test; Mechanical models.

## 1 Introduction

To store and arrange packaged products effectively, warehouses, distribution centers, and industrial facilities frequently use steel pallet racking systems. It is made out of pallet supports or wire mesh decking, horizontal beams, and upright frames. The advantages and typical applications of steel pallet racking systems include Optimized Storage Space: Steel pallet racking systems make effective use of vertical space, enabling companies to store as much inventory as possible. The essential components of steel storage racks are column bases, upright frames, beams, and beam-to-upright connectors. In rack systems, uprights feature a series of holes along their length that enable beams to be attached at different heights. Beams are welded to beam end connectors. Pallet racks are rarely set up with brac-

ings to ensure that palletized items are constantly accessible. On the other hand, plan bracing is utilized on the top level of double-sided high-rise steel pallet racks, and diagonal bracing is often positioned in the back of the rack structure. The stability of the system in plan is achieved by the beam end connector, so it is important to study the behavior of the connection. But it is challenging to forecast the precise flexural behavior of beam-to-upright connections due to the many constructional elements. Consequently, experimental test methods (cantilever test method and/or portal test method) are provided by the current design codes for steel storage racks (Australian Standard AS 4048 [1], the Rack Manufacturers Institute (RMI) [2], and the European Standard EN 15512 [3]) in order to obtain the stiffness and strength requirements for storage rack structural design. Numerous investigators have shared their experimental findings about the flexural behavior of beam-to-upright connections in steel storage racks. Vimal Mohan, J. Rajasankar, and P. Prabha (2015) [4] investigated a single cantilever test, and the experiment examined the rigidity of a pallet rack system. The thickness, upright profile, beam depth, and connector depth were among the parameters that were examined. For thicknesses less than 2.5 mm, failure resulted from the ripping of the upright web on the tension side. Four- or five-tab connections with larger uprights and deeper beams produced stiffer and stronger joints. For beam depths up to 125 mm, the bigger intermediate stiffener in the upright profile had a low impact on moment-bearing capacity. Florin Dumbrava and Camelia Cerbu (2020) [5] studied Three types of beams with varied box cross-section sizes, three types of upright profiles with different section thicknesses, and two types of connectors (four-tab and five-tab) were all tested 101 times for this study. The significance of figuring out the rotational stiffness of the link was highlighted by a numerical analysis. A total of four beam models  $k = 0$  hinged,  $k = \infty$  fixed, and  $k = 35 \text{ KN.m/rad}$ – $102 \text{ KN.m/rad}$  semi-rigid with different rotational stiffness were examined. The results showed how important it was to figure out how stiff these semi-rigid connections were because boundary conditions had a big influence on stresses, bending moments, and deflection. The findings indicated that for uprights with a thickness of 1.50 mm, assemblies with five-tab connections produced higher rotational stiffness and larger design moment values than assemblies with four-tab connectors, and when five-tab connections were used instead of four-tab ones, the rotational stiffness increased but the design moment reduced because of the altered failure modes brought about by the additional thickness. Xianzhong Zhao, Liusi Dai, and Tuo Wang (2017) [6] provided a mechanical model to forecast the initial rotational stiffness of beam-to-upright connections in cold-formed steel storage racks using the component technique. The five fundamental deformable elements in the model tab in bending—the upright wall in bearing, the upright wall in bending, the beam-end connector in bending and shear, and the upright web in shear—are responsible for the initial rotational stiffness of beam-to-upright connections. The initial rotational stiffness of beam-to-upright boltless connections in steel storage racks is investigated theoretically in this article, and a mechanical model based on the component technique is proposed to calculate the initial rotational stiffness of boltless connections, drawing on basic analysis and earlier experimental data. Rodoljub Vujanac, Nenad Miloradovi' and Snežana Vulovi'c [7] tested protocol for the behavior of beam-to-column connections is offered, and the protocol specified in the applicable design codes is used to assess the test results. In order to circumvent costly experiments to ascertain the structural characteristics of various kinds of connections, a polynomial model and matching numerical model were created to serve as experiment simulators. The constructed analytical and numerical model can be used to investigate different beam-to-column connection combinations once it has been verified. Lucjan Ślęczka and Aleksander Kozłowski (2007) [8] demonstrated the use of the component technique to evaluate the moment resistance and initial stiffness of storage rack joints—two major joint

attributes. The outcomes of the tests are compared with the results obtained using the established model. The ability to precisely and clearly specify how each component affects the stiffness and resistance of the joint is one of the benefits of the component technique. It is simple to find and strengthen the weakest link. It facilitates the optimization of joints, particularly in systems like steel storage pallet racks that are manufactured in lengthy series. Hanisha and Kishore [9] compared the experimental analysis results and the finite element analysis results of some specimens, and the results found that even with the same characteristics and load settings, the specimen created in the FEA model yielded 6% lower results than the laboratory value. Florin Dumbrava and Camelia Cerbu [10] studied the effect of the looseness angle on the pallet rack system. They found that the theoretical model was applied to additional kinds of beam-to-upright connections in order to assess the impact of the connection parameters on calculus corrections. It is demonstrated that the maximum corrections for the maximum deflection and the bending moment created at the middle of the beam are, respectively, 2.99% and 5.16%. It has been demonstrated that the type of connector influences the correction's magnitude. Zhi-Jun Lyu and HongLiang Li [11] predicted the bending strength of boltless steel connections in storage pallet racks by experimental and FEM models. Compared to the results produced from the ANN models, the prediction performance of the data-driven model based on SVM technique is considerably closer to the physical test and FEM, indicating that the model is very efficient.

## 2 Experiment test setup and results

Seven beam-to-upright connections were tested at the engineering faculty laboratory at Mattaria-Helwan University using a single cantilever as a recommendation from the EN 15512:2009 code [3]. The specimens took into account three distinct beam sections and four distinct upright perforated sections. The tests constants are the beam end connector, the length of the beam and the height of the upright. The purpose of the single cantilever testing was to determine the connection's initial rotational stiffness ( $K_0$ ). The connection details were specified on the labels of the specimens. For instance, "C80-1.5-B90-1.5" shows a column width of 80mm with a 1.5 mm column thickness and a 90 mm beam height with a 1.5 mm beam thickness. The uprights and the beam sections are shown in Fig 1 and Fig 2, respectively. Regarding the connector, it is invariable with a height 200 mm a thickness 3.0 mm with four hooks (tabs), it is welded to the end of the beam. The connector's nominal dimensions are displayed in Fig 3. All-test specimens are listed in Table 1. In all specimens, the beam and the end connector center lines are in place. But in T7, the beam axis is flushed from the bottom with the connector to test the effect of the position of the beam with the end connector.

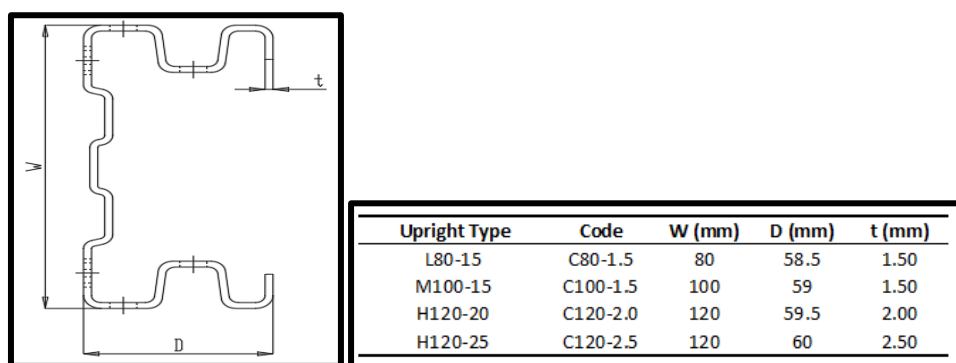


**Fig 1.** The cross-sectional dimensions of the uprights.

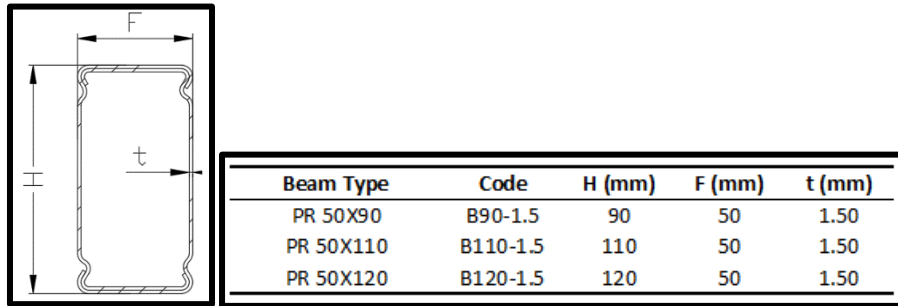


Fig 2. The cross-sectional dimensions of the beams.

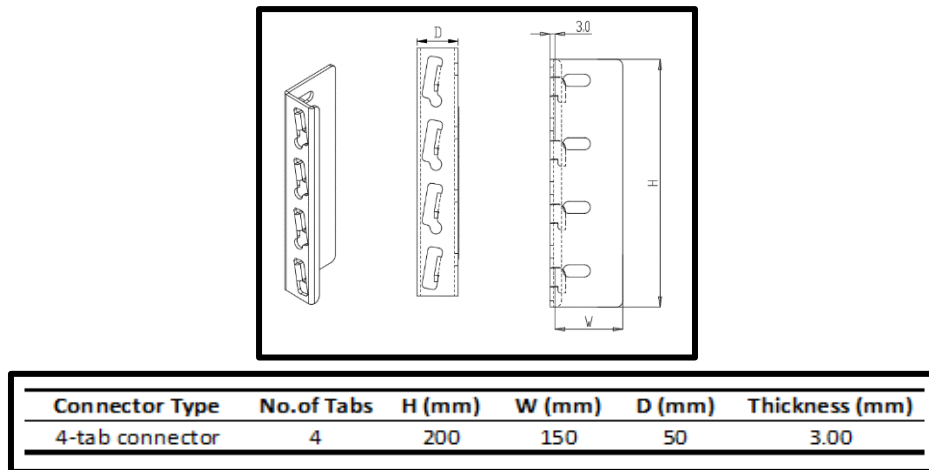
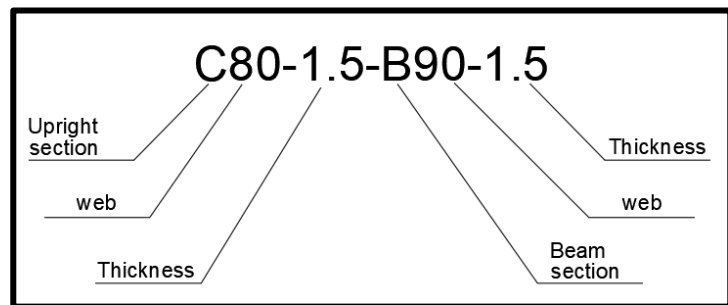


Fig 3. The dimensions and geometry of the beam end connection.

Table 1. Labels used for assembly of experimental specimens.

Assembly labels	Test No.
C80-1.5-B90-1.5	T1
C80-1.5-B120-1.5	T2
C100-1.5-B90-1.5	T3
C120-2.0-B90-1.5	T4
C120-2.0-B120-1.5	T5
C120-2.5-B110-1.5	T6
C100-1.5-B90-1.5 Lower welding the connector	T7



The loading frame with capacity 4000 kN is used in the test. At the bottom flange of the loading frame girder, in line with the center of the loading system, was installed a 1500 kN hydraulic jack with a 100 mm stroke. The load was applied using a load cell that had a capacity of 250 kN and a pressure of 1000 bar with an accuracy of 10 kg. Each upright specimen's top and bottom to secure  $U_x$ ,  $U_y$ , and  $U_z$  by two anchor bolts M50-Gr10.9 with two equal angles L60x6. To prevent the beam at the free end

from shifting out of plane, there are two equal back-to-back 60x6 angles that are separated by 55 mm at 400 mm from the upright faces. The vertical load (10% of the ultimate load) was delivered to the end of the beam specimen, and the load was manually applied at a steady, slow pace, in order to produce a static loading state. A calibrated load cell beneath the jack was used to measure the applied loads. The LVDT system (Linear Variable Differential Transformers) is coupled to three dial gauges, each measuring 100 mm in length and with an accuracy of 0.1 mm. The test setup and testing equipment are shown in Fig.4.

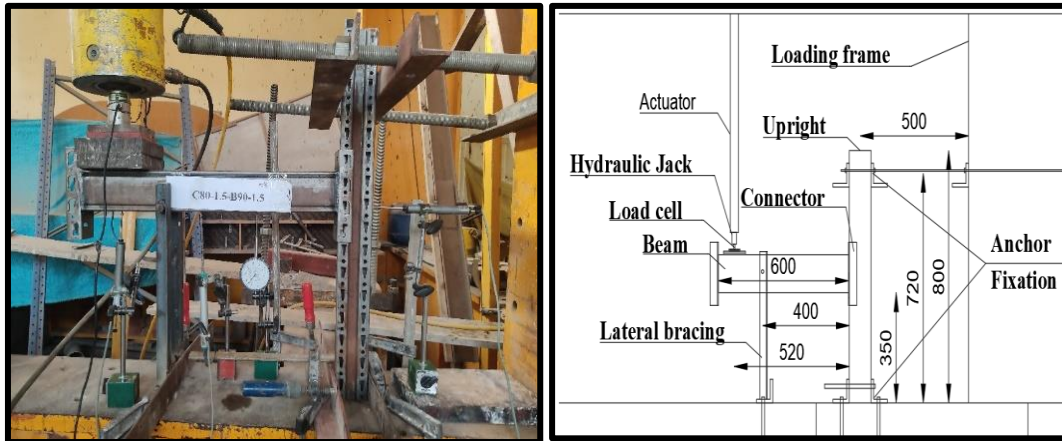


Fig 4. The test setup.

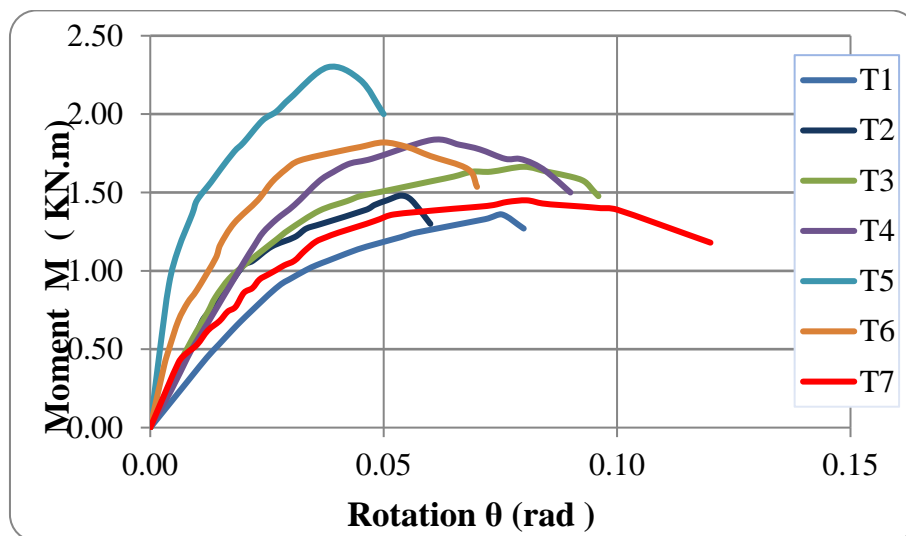


Fig 5. The total (M- $\theta$ ) curve for all specimens

After each test, the (M- $\theta$ ) curve is plotted as viewed in Fig.5, the initial rotational stiffness of the connection is calculated from the curve, and the failure modes are also observed. The specimens most frequently experienced the following failure modes: tearing for the column (TU), warping of the tab end connector (WT), and local buckling for the upright's flange (LB). Table 2 shows the test results, including connection capacity, moment capacity, the corresponding rotational angle, and the failure mode of each test.

According to the EN 15512:2009 code [3], the connection stiffness ( $K_n$ ) of the connection is found by calculating the slope of a line through the origin that divides equal areas ( $A1/A2 \leq 5\%$ ) between that line and the experimental curve below the design moment ( $M_d$ ). And the initial rotational stiffness

( $K_o$ ) of the connection is the initial slope of the ( $M-\Theta$ ) curve, which represents the theoretical stiffness. Fig.6 shows the ( $M-\Theta$ ) curve and the calculated stiffness.

**Table 2.** The examination's results.

Test No.	Specimen label	connection stiffness $K_n$ (kN.m/rad)	Moment capacity $M_f$ (kN.m)	Rotation at $M_f$ $\Theta_f$ (rad)	Failure mode
T1	C80-1.5-B90-1.5	33.63	1.36	0.075	LB & TU
T2	C80-1.5-B120-1.5	60.5	1.48	0.053	WT & LB
T3	C100-1.5-B90-1.5	54.40	1.66	0.08	TU
T4	C120-2.0-B90-1.5	51.72	1.83	0.06	WT
T5	C120-2.0-B120-1.5	68	2.29	0.038	WT & TU
T6	C120-2.5-B110-1.5	62.08	1.82	0.05	WT & TU
T7	C100-1.5-B90-1.5 (LW)	45.76	1.45	0.08	LB & WT

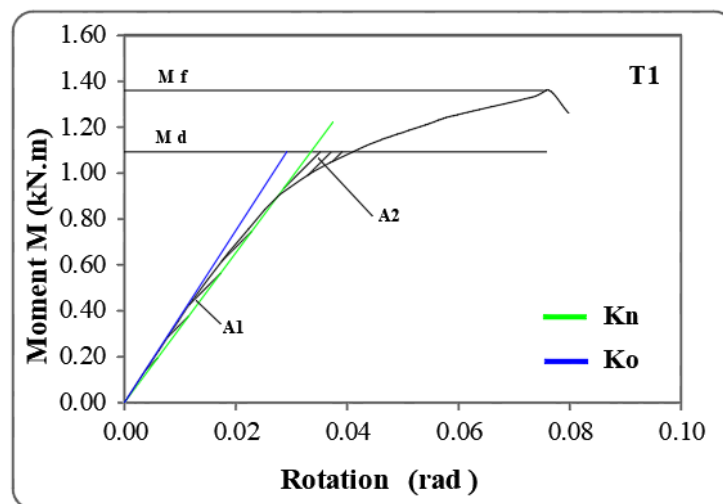


**Fig 6.** As per EN 15512, the rotational stiffness  $K_n$  and  $K_o$  was computed.

### 3 Component Method

In recent years, one of the best techniques for analyzing and forecasting the rotational behavior of various connection types and configurations is the component method. It is mostly applied to steel joints composed of hot-rolled sections and composite joints. For useful design purposes, the mechanical characteristics of steel storage rack beam-to-upright connections were investigated theoretically utilizing the component approaches. As Markazi [12] classified the end connectors into four classes because of their characteristics, in class B (blanking design), which is built into this paper, tabs made by the blanking method interlock with the upright's web either parallelly or perpendicularly. The application of the component method typically involves three main phases. Initially, the process begins with identifying the components within the joint under analysis, where the complex joint is divided into its

constituent parts. Subsequently, each identified component is assessed individually to predict its initial stiffness, strength, and often its deformation capacity. The behavior of each component is typically characterized by a bilinear relationship between displacement and force. Components that do not significantly influence the joint's stiffness are typically modeled as rigid-plastic elements, while other components are represented as elastic-plastic elements. The final stage entails evaluating the flexural strength and rotational stiffness of the entire joint. During this phase, the lever arms are also estimated for each group of components. The behavior of the connection is then forecasted by analyzing groups of springs with axial stiffness, arranged either in series or in parallel. X. Zhao and K. S. Sivakumaran [6] developed a theoretical model aimed at predicting the initial stiffness. Their study delved into the behavior of individual components in the following manner:

### 3.1 The stiffness of the spring for tabs under bending ( $K_{tb}$ ).

During the initial loading phases, tabs, which are fashioned from the beam-end connector, serve as the sole mechanism for transmitting forces from the beam-end connection to the upright. A comparable beam model is employed to illustrate how tabs behave when subjected to bending forces.

$$K_{tb} = \frac{3EI}{l_t^2 \times (l_t + 3l_o)} \tag{1}$$

$$I = \frac{h_t x t_t^3}{12} \tag{2}$$

Where: -

$l_t$  = the connection's side view of the tab end's length,

$l_o$  = the connection's front view of the tab end's length (see in Fig.7)

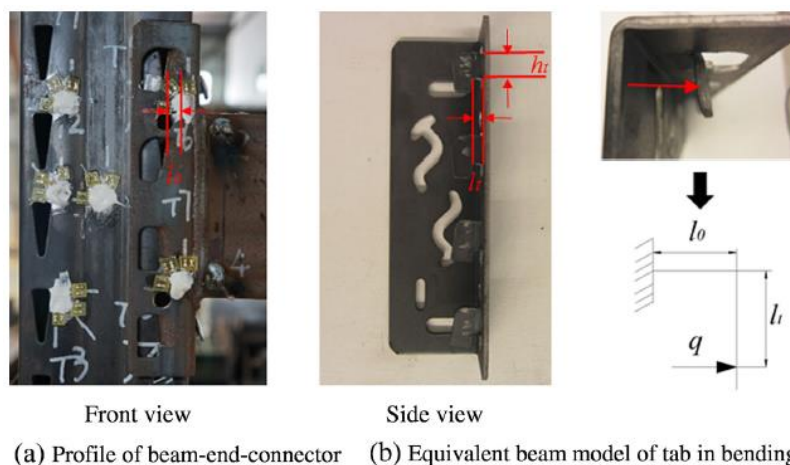


Fig 7. The simplified tab model for bending.

### 3.2 The stiffness of the spring for the upright wall under bearing ( $K_{cwc}$ ).

The stiffness of the spring for the upright wall in bearing ( $K_{cwc}$ ) is determined using the following formula, considering that the perforations of an upright wall in contact with tabs are subjected to a distributed load  $q$  from the tabs. Given that the applied load's inclined angle is negligible, it is presumed to be horizontal.

(3)

$$K_{cwc} = \frac{Eh_t t_{up}}{d_h}$$

Where: -

$t_{up}$  = the upright's thickness,

$d_h$  = the separation between the reaction regions' edge and the loading point of the resultant force. (see Fig.8)

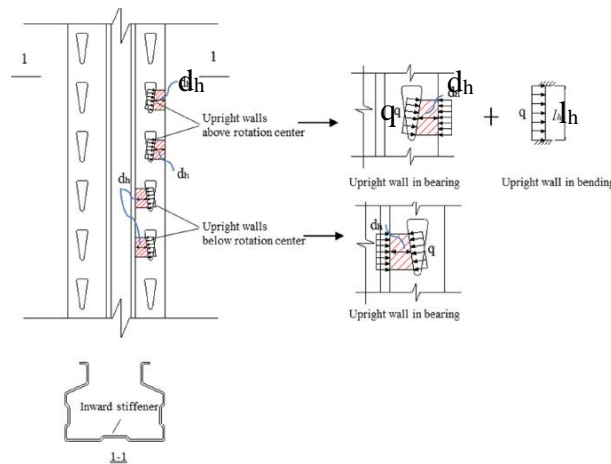


Fig 8. The upright wall behaves under bending and bearing.

### 3.3 The stiffness of the spring for the upright wall under bending ( $K_{cwb}$ ).

For upright walls located below the rotating center, the response to a distributed force transmitted through tabs primarily involves bearing deformation. This is due to the stiffening effect of the column web, which renders bending deformation insignificant in this scenario.

(4)

$$K_{cwb} = \frac{384EI}{l_h^3}$$

$$I = \frac{t_{up} \times d_h^3}{12} \tag{5}$$

### 3.4 Equivalent extensional spring stiffness ( $K_i$ ).

The mechanical model illustrated in Fig 9, along with the formulas used to determine the extensional stiffness of each fundamental component, enable the accurate calculation of the initial rotational stiff-



ness of steel storage rack beam-to-upright connections by combining the stiffness values of these individual components.

The procedures for calculating the initial rotational stiffness of the connection are depicted in Fig.10. Equation (6) provides the formula for evaluating the stiffness of a corresponding extensional spring, denoted as  $K_i$ , where "i" represents the number of tab rows.

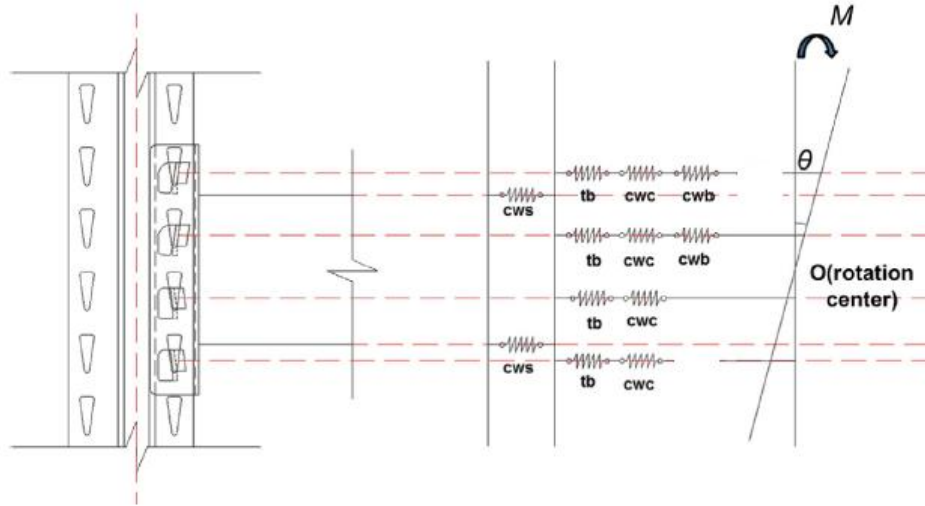


Fig 9. The four tabs' mechanical model.

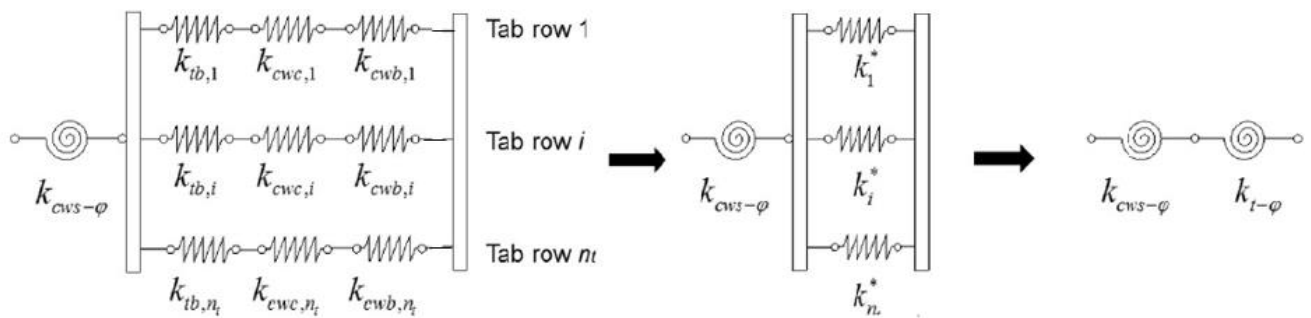


Fig 10. Technique for figuring of the starting stiffness during rotation.

$$K_i = \frac{1}{\frac{1}{K_{tbi}} + \frac{1}{K_{cwc_i}} + \frac{1}{K_{cwb_i}}} \tag{6}$$

### 3.5 Stiffness of upright web in shear ( $K_{cws-\Phi}$ ).

The axial stress arising from the column's axial load is neglected according to the fundamental assumptions of the model. Considering the minor moment-induced deflection of the selected web panel, it can be simplified as a plate experiencing pure shear stress. The axial stiffness, denoted as  $K_{cws-\Phi}$ , of the equivalent spring depicted in Fig 11, is calculated by employing Equation (7).

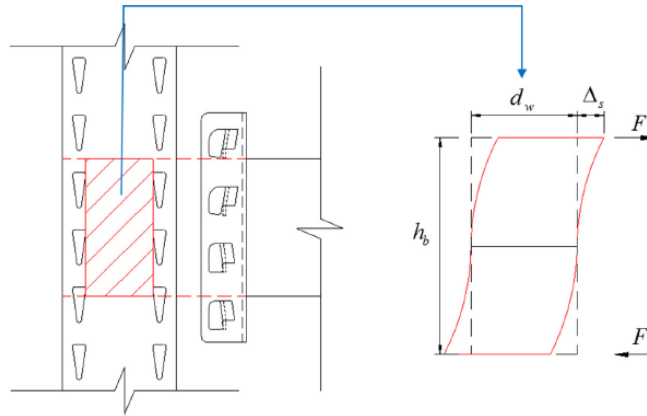


Fig 11. Distortion caused by shearing in the vertical web panel.

(7)

$$K_{cws-\phi} = G t_{up} d_w h_b$$

Where: -

$$G = \frac{E}{2(1 + \nu)} \text{ (shear modulus)}$$

$d_w$ : the web panel's width.

$h_b$ : the beam's height.

### 3.6 Predicted value of initial rotational stiffness ( $K_o$ ).

The corresponding overall rotational stiffness,  $K_{t-\phi}$ , is determined using the following relationship.

$$K_{t-\phi} = \sum_{i=1}^n K_i x L_i^2 \tag{8}$$

The following equation is ultimately used to calculate the initial rotational stiffness of the steel storage rack beam-to-upright connection ( $K_o$ ). It does this by combining the stiffness of the components that are independent of the tab rows, such as the column web in shear (cws), with the equivalent overall rotational stiffness of  $K_{t-\phi}$  that is related to the tab rows.

$$K_o = \frac{1}{\frac{1}{K_{t-\phi}} + \frac{1}{K_{cws-\phi}}} \text{ (predicted value)} \tag{9}$$

The initial rotational stiffness, denoted by the symbol  $K_o$ , is indicated by the slope of the elastic range in the moment-rotation equations.

### 3.7 Validation of the mechanical model with experimental data.

To validate the current component-based mechanical model, the initial rotational stiffness produced from the theoretical model is compared with the available experimental data from the prior single cantilever test.

Table 1 presents the experimental initial rotational stiffness ( $K_e$ ) and theoretical starting rotational stiffness ( $K_o$ ) of the specimens under study, along with the ratio of  $K_o$  to  $K_e$ . It also displays several statistical parameters for  $K_o/K_e$ , including maximum, minimum, average, and standard deviation. These results are significant: the average  $K_o/K_e$  ratio is approximately 1.2, with a standard deviation of 0.16.

**Table 3** The comparison is made between the initial rotational stiffness values obtained experimentally and those projected theoretically.

Test No.	Specimen label	( $K_o$ ) (kN.m/rad)	( $K_e$ ) (kN.m/rad)	$K_o/K_e$
T1	C80-1.5-B90-1.5	42	37.93	1.11
T2	C80-1.5-B120-1.5	86	69	1.25
T3	C100-1.5-B90-1.5	81	68	1.19
T4	C120-2.0-B90-1.5	66	54	1.22
T5	C120-2.0-B120-1.5	89	72	1.24
T6	C120-2.5-B110-1.5	77	65.73	1.17
Maximum				1.25
Minimum				1.11
Average				1.20
Standard deviation				0.16

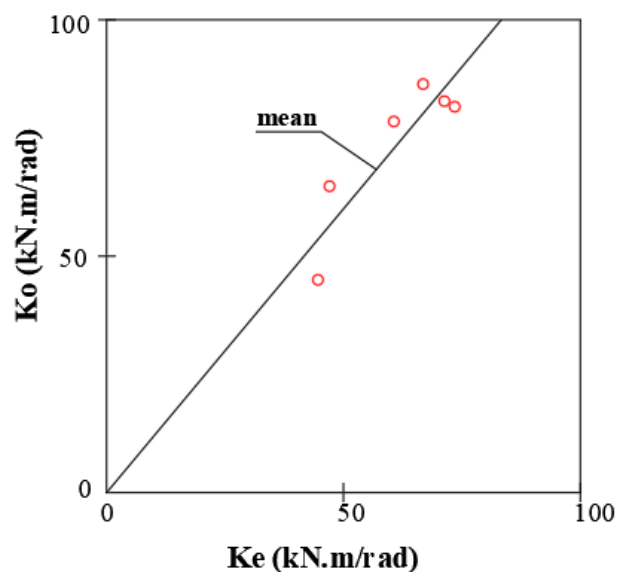


**Fig 12.** The values of initial rotational stiffness, obtained theoretically and experimentally, are compared.

## 4 Conclusion

This paper undertakes a theoretical inquiry into the initial rotational stiffness of beam-to-upright boltless connections in steel storage racks. Leveraging prior experimental findings and fundamental analyses, the paper introduces a mechanical model grounded in the component method. This model serves to compute the initial rotational stiffness of boltless connections. Tab in bending (tb), upright wall in bearing (cwc), upright wall in bending (cwb), and upright web in shear (cws) are the four basic deformable components that are included in the model. The theoretical computation of the extensional stiffness related to each fundamental component is also provided in the study. A comparison of the experimental results and the initial rotational stiffness obtained from the mechanical model is also shown in the publication. The results show that the suggested mechanical model evaluates boltless connections' initial rotational stiffness in steel storage racks in an efficient manner.

The suggested model's main goal is to precisely calculate the beam-to-upright connections in steel storage racks' initial rotational stiffness. It is important to recognize that the initial stiffness, which is specified by the model, limits the connection stiffness. At design stage by any finite element, the predicted initial stiffness can be used with factor of safety.

## References

- [1] AS 4048-Steel Storage Racking, Standards Australia, Australia, 2012.
- [2] RMI. Specification for the Design, Testing and Utilization of Industrial Steel Storage, ANSI, America, 2012.
- [3] EN15512, Steel static storage systems-adjustable pallet racking systems-principles for structural design, UK, 2009.
- [4] Nagendiran, V. Mohan, P.Prabha, J.Rajasankar, N. R. Iyer and N.Raviswaran, "Cold-formed steel pallet rack connection: an experimental study," *Springerlink.com*, pp. 55-68, 2015.
- [5] Florin Dumbrava and Camelia Cerbu, "Experimental Study on the Stiffness of Steel Beam-to-Upright Connections for Storage Racking Systems," *materials*, pp. 1-27, 2020.
- [6] X. Zhao, L. Dai, TuoWang, K. S. Sivakumaran and Y. Chen, "A theoretical model for the rotational stiffness of storage rack," *Journal of Constructional Steel Research*, vol. 133, pp. 269-281, 2017.
- [7] R. Vujanac, N. Miloradovi and A. Pavlovic, "A Comprehensive Study into the Boltless Connections of Racking Systems," *metals*, 2020.
- [8] Kozłowski, L. Ślęczka and Aleksander, "Experimental and theoretical investigations of pallet racks connections," *Advanced Steel Construction*, vol. 3, pp. 607-627, 2007.
- [9] C. S. S. Hanisha and I. S. Kishore, "Experimental and finite element analysis of cold formed steel beam-column joint," *Materials Today: Proceedings*, 2020.

- [10] F. Dumbrava and C. Cerbu, "Effect of the Looseness of the Beam End Connection Used for the Pallet Racking Storage Systems, on the Mechanical Behavior of the Bearing Beams," *materials*, 2022.
- [11] Z.-J. Lyu, P. Zhao and H. Li, "Prediction of the Bending Strength of Boltless Steel Connections in Storage Pallet Racks: An Integrated Experimental-FEM-SVM Methodology," *Hindawi*, 2020.
- [12] Markazi, Beale and Godley, "Experimental Analysis of Semi-Rigid Boltless Connectors," *Thin-Walled Structure*, pp. 57-87, 1997.
- [13] L. Alves, G. Cássio and A. Neiva, "Analysis of beam to upright end connection steel storage systems," *Advanced Steel Construction*, vol. III, p. 279–286, 2020.
- [14] O. Bové, M. Casafont and J. Bonada, "Comparison between numerical models for unbraced multiple bay pallet racks," *euro steel*, 2023.
- [15] O. Bove, F. L'opez-Almansa and M. Ferrer, "Ductility improvement of adjustable pallet rack speed-lock connections Experimental study," *Journal of Constructional Steel Research*, 2022.